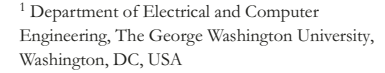
ORIGINAL RESEARCH PAPER



Optimal integration of interconnected water and electricity networks





² Electrical Engineering Department, College of Engineering, King Saud University, Riyadh, Saudi Arabia

Correspondence

Payman Dehghanian, Department of Electrical and Computer Engineering, The George Washington University, Washington DC, USA. Email: payman@gwu.edu

Abstract

With the widespread deployment of advanced heterogeneous technologies and growing complexity in our modern society, there is an increasing demand for risk-aware management and joint operation of interconnected infrastructures and lifeline networks. The coordination between Power and Water Networks (PWNs) is urgently needed as water networks are one of the most energyintensive critical infrastructures. This paper proposes a framework for day-ahead operation optimization and coordination of the interconnected Joint Power and Water Networks (JPWNs). Unlike the state-of-the-art where PWNs are individually operated in their respective domains, we present an integrated framework for PWNs that conjoins the Optimal Power Flow (OPF) mechanisms in power grids with innovative operation models of the water networks. Piece-wise linearization is applied to the nonlinear hydraulic operating constraints to convert the proposed optimization model into a mixedinteger linear programming (MILP) formulation. The suggested framework is applied to a 15-node water network jointly operated with the IEEE 9-bus and IEEE 57-bus test power systems. The simulation results show the effectiveness of the proposed framework, resulting in cost reduction and energy-saving when both systems' operation is jointly optimized. The results show that the proposed methodology is scalable and computationally-efficient when applied to larger-scale systems.

INTRODUCTION

Water and energy are the two most critical lifeline infrastructures as they play central roles in back-boning modern society and human life. Electricity usage for pumping water through water systems accounts for a high percentage of the total electricity demand globally [1]. The electricity consumption by water infrastructure alone is approximated around 4% of the total electricity consumption in the United States [2]. The projected ramping of the populations in modern societies calls for further electrification of the Power and Water Networks (PWNs) in the next years to come; therefore, there is an urgent need for improved reliability and efficiency of the water networks and the water facilities, that is, water treatment, water purification, cooling, wastewater etc.

While water and power systems have traditionally been designed and planned as two independent and uncoupled

systems, they need to be operated jointly and interdependently in real-world applications [3]. Water facilities need to be delivered electricity from power systems to normally and adequately operate. On the other hand, water is essential for refining fuels and generating electricity. With the apparent interdependency of power and water systems, a challenging concern exists in the scenarios of limited availability in either water or electricity. For instance, in the case where a shortage in cooling water for conventional steam power plants is realized, water system may not be supplied with sufficient amount of electricity needed to pump the water through transmission pipelines; this could, in turn, lead to a failure in both systems. The closely intertwined PWNs ecosystem is commonly referred to as waterenergy nexus (WEN) [4-6].

WEN has been widely investigated in the literature. The effects of climate change on the operation of hydro power plants and water reservoir management were studied in [7].

This is an open access article under the terms of the Creative Commons Attribution License, which permits use, distribution and reproduction in any medium, provided the original work is properly cited.

© 2021 The Authors, IET Generation, Transmission & Distribution published by John Wiley & Sons Ltd on behalf of The Institution of Engineering and Technology

Reference [8] provides a literature review on the water system optimization with special considerations to WEN. WEN linkage analysis is employed in [9] to demonstrate the impacts of considering coupled water-power networks on different economic sectors. Effects of the battery storage facilities on the optimal dispatch of power and water in WENs are studied in [10]. A power and water economic dispatch approach for the supply side has been developed in [6]. Reference [11] presents a mathematical co-dispatch model for the optimal network flows in both water and power systems. Daily hydro-thermal operation scheduling using robust optimization is investigated in [12], taking into consideration only water network constraints while ignoring those of the power transmission networks. Different techniques using physics-based modeling of WEN are suggested in [13] to model the interdependence structure of water, wastewater, and power systems. Demand response and frequency regulation for water distribution systems is studied in [14]. Energy flexibility through the coordination of water and power systems is introduced in [15]. Multi-objective optimization for PWNs operation under the uncertainty of river inflows is introduced in [16]. A methodology to assess the infrastructural and operational resilience of PWNs under limited water and/or energy availability is presented in [17]. Another scope of research in this area focuses on cost minimization using strategies for load management in water and wastewater sectors and on the efficiency of passive energy to help maintain the power grid's reliability [18-20]. Economic impact of the electricity demand of the water facilities on power system operation using different energy efficiency programs is explored in [21]. The use of renewable energy sources in the operation of PWNs is investigated in [22–24]. References [23, 24] proposed a model for utilizing solar energy in PWNs. A framework for utilizing water pumps and tanks to receive the needed electricity for their operation from renewable sources is presented in [22]. The coordination between water and electricity networks is investigated in [25]. A mathematical co-dispatch approach to achieve the optimal network flows in PWNs is studied in [26]. Reference [27] investigated the demand forecast errors in the operation of PWNs. Uncertainty modeling of the WEN is investigated in [28, 29]. A scenario approach is used in [28] to model the uncertainty of water demand forecasts, while [29] proposed a two-stage distributionally robust operation model for the WEN

Focusing only on the operation of water pumps and excluding the power system constraints has also been a wide and common area of research in the literature [30, 31]; studies to model and integrate the interactions between the water and power systems are found scarce. Modeling such interactions and interdependencies is critical as separate management of the two networks individually will result in sub-optimal solutions in one another. Examples of such sub-optimal solution can be found in many references in the literature where the first optimization procedure focuses solely on water networks that provide the electricity consumption of the water facilities to power system operators, and the second optimization model is managed by power system operators considering the submitted electric-

ity demand by water network infrastructure. This will result in a lack of coordination between the two systems which, in turn, may lead to a shortage of water demand and/or essential water used for refining fuels and electricity generation. Additionally, the computational time to continuously coordinate the water and power systems would be challenging, particularly during emergency operating conditions. Furthermore, this coordination relies heavily on reliable and secure communication networks across the WEN landscape, where a failure, latency, or attack may compromise the reliability and dependability of the two systems. Such lack of coordination was experienced during the Maria hurricane in Puerto Rico [32], where hurricane damaged around 90% of the state's electrical system, and large areas were not supplied with water for a long time due to the severance of the hurricane and the lack of coordination between different interconnected sectors, that is, power and water operators, which resulted in a longer recovery time [33, 34].

Different from the traditional practices where the operation of power and water networks has been approached either independently or coordinated through an iterative exchange of status information between the networks—yet vulnerable to communication latencies, cyber-attacks, and sub-optimal solutions—, this paper bridges the gap by introducing novel techniques for the operation of the Joint Power-Water Networks (JPWNs). To the best of the authors' knowledge, a holistic framework for modeling and co-optimizing of the interdependent PWNs is missing in the literature. The presented model aims to enhance the flexibility of both electric and water systems and elevates the efficiency and resiliency of both systems in the face of severe disruptions. The proposed framework dynamically receives the input information from both networks and minimizes the energy consumption of the intensive water network infrastructure, for example, pumps (see Figure 1). The forecasted dayahead demanded water, as well as electricity prices, are employed to minimize the total operation cost of both systems.

The rest of the paper is organized as follows. Section 2 introduces the proposed integrated optimization framework for JPWNs, considering DC optimal power flow (DCOPF) and AC optimal power flow (ACOPF) mechanisms. Numerical case studies and simulation results on a 9-bus test system integrated with three 15-node water networks is presented in Section 3. The paper is eventually concluded in Section 4.

2 | PROPOSED METHODOLOGY

In this section, the proposed formulation for the integrated modeling and optimization of JPWNs is presented. The components of the water network (e.g. reservoirs, pipes, pumps, and tanks) are mathematically modeled based on the a directed graph $G=(N,\mathcal{A})$, that is, a set of nodes connected together by arcs directed from one node to another, where N represents the set of water system nodes consisting of water sources (i.e. reservoirs or tanks) or customers demand. Pipes j and pumps p are represented by \mathcal{A} , where $\mathcal{A}=\{p\cup j\}$. Positive and negative values for the water flow rate \mathcal{Q} define the direction of each

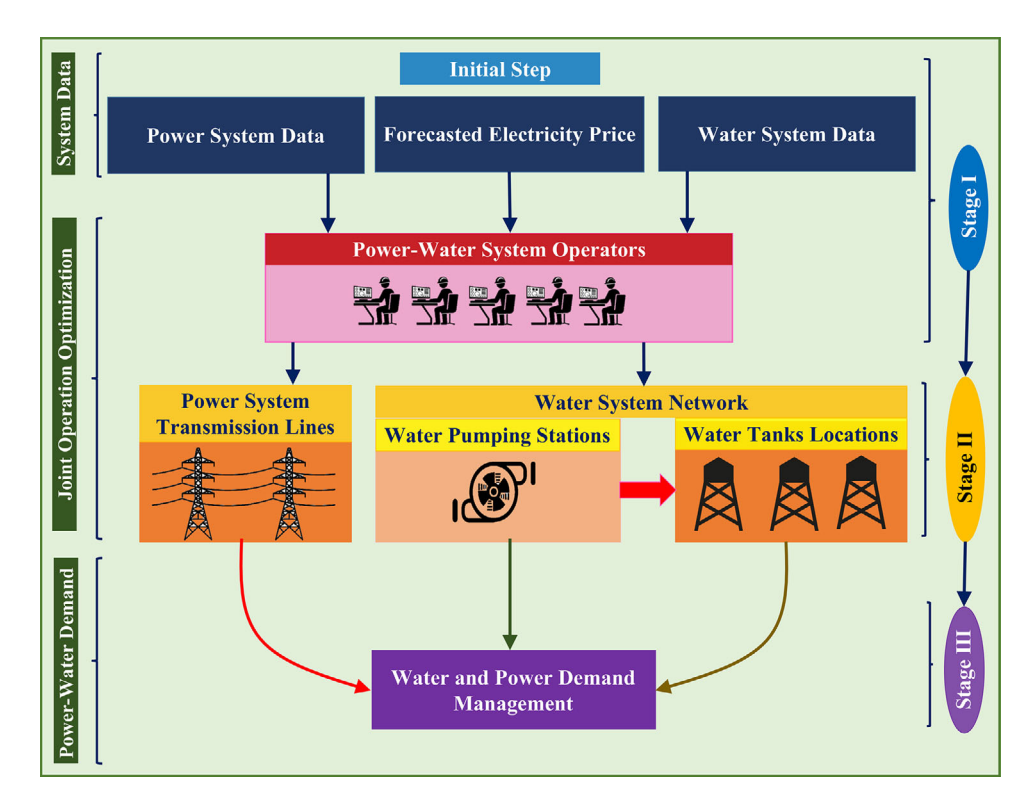


FIGURE 1 General architecture of the proposed framework for joint operation optimization of interdependent power systems and water networks

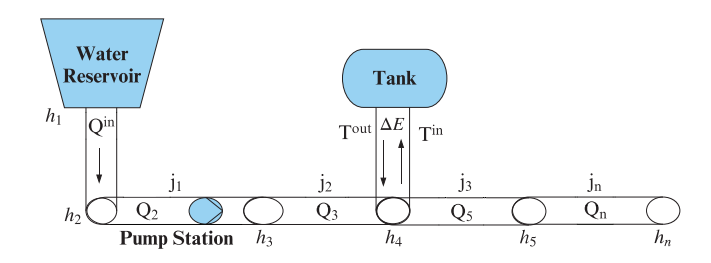


FIGURE 2 Schematic diagram of a typical water network

arc. The schematic diagram of a water system and its hydraulic components are illustrated in Figure 2.

2.1 Water flow balance constraints

Water system demand is delivered to consumers from the reservoirs and tanks through a network of pipes and pumps. The water flow balance constraints are modeled as follows:

$$Q_{b,t}^{in} - D_{b,t} - Q_{b,t} - \Delta E_{b,t} = 0 \qquad \forall b, \forall t, \qquad (1a)$$

$$\Delta E_{b,t} = T_{b,t}^{in} - T_{b,t}^{out} \qquad \forall b, \forall t, \tag{1b}$$

$$-Q_{\max,b}^{j} \le Q_{b,t}^{j} \le Q_{\max,b}^{j} \qquad \forall b, \forall t, \qquad (1c)$$

$$Q_{b,t}^{p} \ge 0 \qquad \forall b, \forall t, \tag{1d}$$

$$Q_{b,t}^{in} \ge 0 \qquad \forall b, \forall t. \tag{1e}$$

Water flow balance equation in the water network is modeled in (1a). The difference between the input and output water flow of the tank $\Delta E_{b,t}$ is modeled in (1b), while the water flow through pipes $Qj_{b,t}$ is limited in (1c). Water flow through pumps is bounded in constraint (1d). Constraint (1e) ensures that only positive values can be taken for the reservoirs' nodes.

2.2 | Nodal pressure head models for pipes

Water flows through pipes j are resulted by the pressure level difference between the water nodes N. The nodal pressure head for pipes is modeled as follows:

$$b_{n,h,t}^{j} - b_{n+1,h,t}^{j} = r_{p} | Q_{h,t}^{j} |^{1.852} Sign(Q_{h,t}^{j}) \quad \forall b, \forall t,$$
 (2a)

$$r_p = \frac{8L_p}{\pi^2 g d_p^2},\tag{2b}$$

$$b_{b,t}^{r} - \hat{b}_{b} = 0 \qquad \forall t, \forall b, \qquad (2c)$$

$$b_{min,b} \le b_{b,t} \le b_{max,b}$$
 $\forall t, \forall b.$ (2d)

The flow of water through pipes is modeled in (2a) by the Hazen–Williams formula, where the coefficient r_p depends only on the water flow as presented in (2b). Pressure head of the water reservoirs are fixed by its geographical heights in (2c), as reservoirs are considered unlimited sources of water. Constraint

(2d) bounds the nodal pressure in water networks. A piece-wise linear formulation [14, 35] is applied to guarantee a feasible solution of the optimization problem. This is because constraint (2a) is, in nature, a polynomial nonlinear function. In large scale systems, the nonlinear model may not result in a global optimal solution. In order to apply the piece-wise linearization, $Q_{b,t}^j$ is divided into several breakpoints $(q_1^j, q_2^j, \dots, q_I^j)$. q_1^j and q_1^j are set at the extremes (i.e. at the maximum and minimum values of $Q_{b,t}^j$). Let $Y_{b,t}^{i,j}$ be a binary variable for each pipe at each bus which is associated with the *i*th interval (i.e. q_i^j, q_{i+1}^j). Note that $Q_{b,t}^j$ is forced to be associated with a pair of consecutive breakpoints where $X_{b,t}^{i,j} \in [0,1]$ is introduced as a continuous variable for each breakpoint. Dummy parameters are introduced such that $Y_0 = Y_n = 0$. Finally, the pressure head difference $\Delta b_{b,t}^j(q_i^j)$ can be approximated through the following set of constraints:

$$\sum_{i=1}^{I-1} Y_{b,t}^{i,j} = 1 \qquad \forall b, \forall j, \forall t, \tag{3a}$$

$$X_{b,t}^{i,j} \le Y_{b,t}^{i-1,j} + Y_{b,t}^{i,j} \qquad \forall b, \forall j, \forall i, \forall t,$$
 (3b)

$$\sum_{i=1}^{I} X_{b,t}^{i,j} = 1 \qquad \forall b, \forall j, \forall t, \qquad (3c)$$

$$X_{b,t}^{I,j} \le Y_{b,t}^{I-1,j} \qquad \forall b, \forall j, \forall t, \tag{3d}$$

$$X_{b,t}^{1,j} \le Y_{b,t}^{1,j} \qquad \forall b, \forall j, \forall t, \tag{3e}$$

$$Q_{b,t}^{j} = \sum_{i=1}^{I} X_{b,t}^{i,j} q_{i,b}^{j} \qquad \forall b, \forall j, \forall t,$$
 (3f)

$$b_{n,b,t}^{j} - b_{n+1,b,t}^{j} = \sum_{i=1}^{I} X_{b,t}^{i,j} \Delta b_{b,t}^{j} (q_{i}^{j}) \qquad \forall b, \forall j, \forall t.$$
 (3g)

Constraint (3a) enforces only one binary variable to take the value of 1, while (3b)–(3e) imply that only values other than zero are chosen for $X_{b,t}^{i,j}$ and $X_{b,t}^{i+1,j}$. Constraints (3f)–(3g) ensure that the pressure difference for each pipe is properly chosen to accurately assess the approximated values.

2.3 | Tank and pump operation constraints

Tanks and pumps are the most challenging components to be modeled in the water networks. Tank is used to smoothen the pumpage demands during peak hours and to assist the water network during the emergency conditions. Water tank's dynamic operation is modeled as follows:

$$V_{b,t+1} = V_{b,t} + \Delta E_{b,t} \qquad \forall b, \forall t, \tag{4a}$$

$$V_{ht} = S_a h_{ht} \qquad \forall b, \forall t, \tag{4b}$$

$$V_{min,b} \le V_{b,t} \le V_{max,b}$$
 $\forall b, \forall t,$ (4c)

$$\Delta E_{min,b} \le \Delta E_{b,t} \le \Delta E_{max,b}$$
 $\forall b, \forall t.$ (4d)

The flow balance equation for tanks is modeled in constraint (4a). The pressure head at tank nodes is driven by the water stored in the related tanks, as formulated in (4b). Constraint (4c) limits the volume of each tank to its minimum and maximum capacity. The difference between the charging and discharging water flow in tanks is limited in constraint (4d). Water pump (p) increases the pressure $\Delta b_{b,t}^p$ by a controlled positive amount (i.e. $\Delta b_{b,t}^p = b_{n+1,b,t}^p - b_{n,b,t}^p$). The increase in water pump pressure is modeled in (5a). The electricity consumption for each pump is formulated in (5b) and the pump electricity consumption is limited in (5c).

$$\Delta h_{b,t}^{p} = W_{b,t} \left(a_1 - a_2 \left(\frac{Q_{b,t}}{W_{b,t}} \right)^{a_3} \right) \qquad \forall b, \forall t, \quad (5a)$$

$$P_{b,t}^{p} = W_{b,t}^{3} \left(b_1 - b_2 \left(\frac{Q_{b,t}}{W_{b,t}} \right) \right) \qquad \forall b, \forall t, \qquad (5b)$$

$$P_{\min h}^{p} \le P_{h t}^{p} \le P_{\max h}^{p} \qquad \forall b, \forall t. \tag{5c}$$

Non-linearity is present in the water pressure equations for pump and pump power consumption constraints (5b) and (5c), respectively. The triangle technique is used to approximate the bi-variate functions $\Delta b_{b,t}^p$ and $P_{b,t}^p$. First, breakpoints are selected by dividing the x and y axes, respectively, into U and M points (i.e. $q_{1,b}^p, q_{2,b}^p, \dots, q_{U,b}^p, w_{1,b}^p, w_{2,b}^p, \dots, w_{M,b}^p$). The breakpoints $(q_{1,b}^p, q_{U,b}^p)$ and $(w_{1,b}^p, w_{M,b}^p)$ represent the minimum and maximum water flows through pump $\mathcal{Q}_{b,t}^p$ and speed of pump $W_{b,t}$, respectively. Continuous variable $X_{b,t}^{u,m,p} \in [0,1]$ associated with each (u,m) is introduced. Also, dummy variables for all upper and lower binary β have to be set to zero such that $\beta_{0,*}^{Upper} = \beta_{*,0,*}^{Upper} = \beta_{*,0,*}^{Upper} = \beta_{*,0,*}^{Upper} = 0$ and $\beta_{0,*}^{Lower} = \beta_{*,0,*}^{Lower} = \beta_{*,0,*}^{L$

$$\sum_{n=1}^{U} \sum_{m=1}^{M} X_{b,t}^{n,m,p} = 1 \qquad \forall p, \forall b, \forall t, \qquad (6a)$$

$$Q_{b,t}^{p} = \sum_{u=1}^{U} \sum_{m=1}^{M} X_{b,t}^{u,m,p} q_{u,b}^{p} \qquad \forall p, \forall b, \forall t,$$
 (6b)

$$W_{b,t} = \sum_{u=1}^{U} \sum_{m=1}^{M} X_{b,t}^{u,m,p} u_{m,b}^{p} \qquad \forall p, \forall b, \forall t,$$
 (6c)

$$\Delta h_{b,t}^{p} = \sum_{u=1}^{U} \sum_{m=1}^{M} \Delta h_{b,t}^{p} (q_{u,b}^{p}, u_{m,b}^{p}) X_{b,t}^{u,m,p} \quad \forall p, \forall b, \forall t, \quad (6d)$$

$$P_{b,t}^{p} = \sum_{u=1}^{U} \sum_{m=1}^{M} P_{b,t}^{p}(q_{u,b}^{p}, w_{m,b}^{p}) X_{b,t}^{u,m,p} \qquad \forall p, \forall b, \forall t,$$
 (6e)

$$\sum_{u=1}^{U} \sum_{m=1}^{M} \left(\beta_{u,m,p,b,t}^{Upper} + \beta_{u,m,p,b,t}^{Lower} \right) = 1 \qquad \forall p, \forall b, \forall t,$$
 (6f)

$$\begin{split} X_{b,t}^{u,m,p} &\leq \beta_{u,m-1,p,b,t}^{Upper} + \beta_{u+1,m,p,b,t}^{Upper} + \beta_{u,m,p,b,t}^{Upper} \\ &+ \beta_{u-1,m,p,b,t}^{Lower} + \beta_{u,m+1,p,b,t}^{Lower} \\ &+ \beta_{u,m,p,b,t}^{Lower} & \forall u, \forall m, \forall p, \forall b, \forall t. \end{split}$$

The weights of the convex combination for the selected triangle is introduced in (6a). Constraints (6b) and (6c) represent the linear combinations of any values for $Q_{b,t}^{p}$ and $W_{b,t}$, respectively. The bi-variate nonlinear functions for the pressure difference in each water pump $(\Delta b_{b,t}^{p})$ and the power consumption of pumps $(P_{b,t}^{p})$ are approximated in (6d) and (6e), respectively. Constraint (6f) ensures that only one triangle is used for the convex combination. Constraint (6g) enforces that only non-zero values of $X_{b,t}^{i,m,p}$ can be associated with the three vertices of the triangle.

2.4 Water-power network integration constraints

2.4.1 | DCOPF

Power system's DC optimal power flow (DCOPF) mechanism is integrated with the water network through the following constraints.

$$P_{b,t}^{p,new} = \sum_{t=1}^{P} B P_{b,t}^{p} \qquad \forall b, \forall t, \tag{7a}$$

$$P_{dn,t} = P_{d,t} + P_{h,t}^{p,new} \qquad \forall n, \forall t, \tag{7b}$$

$$\underline{P_{dn}} \le P_{d,t} + P_{b,t}^{p,new} \le \overline{P_{dn}} \qquad \forall n, \forall t, \tag{7c}$$

$$\sum_{g=1}^{G} P_{g,t} - \sum_{m \in \Omega_{t}^{n}} P_{knm,t} = P_{dn,t} \qquad \forall n, \forall t, \qquad (7d)$$

$$P_{k,t} = \frac{\theta_n - \theta_{m,t}}{x_k} \qquad \forall k, \forall t, \tag{7e}$$

$$-P_{k}^{max} \le P_{knm,t} \le P_{k}^{max} \qquad \forall k, \forall t, \tag{7f}$$

$$p_g^{min} \le P_{g,t} \le P_g^{max} \qquad \forall t. \tag{7g}$$

A new parameter for pump power consumption is introduced in (7a) to adjust the dimension of $P_{b,t}^{p}$. Constraint (7b) sums the total electricity demand for power and water networks together. Electricity consumption is bounded in (7c).

Power balance constraint at each bus is enforced in (7d). Constraint (7e) sets the power flow in transmission lines. The power flow in each transmission line is bounded to the minimum and maximum limits in (7f). Output power of system generating units is limited to the minimum and maximum capacities in (7g). The complete mixed-integer linear programming (MILP) optimization model for the joint operation of power grids integrated with water networks is formulated below:

$$\min \sum_{t=1}^{NT} \sum_{p=1}^{G} \sum_{r=1}^{\mathbf{R}} \sum_{b=1}^{\mathbf{P}} \left(c_{0,t} + c_{g,t} P_{g,t} + c_{p,t} P_{b,t}^{b} + c_{r,t} Q_{b,t}^{in} \right)$$

subject to (1a - 1d), (2c - 4d), (5c - 6g), (7a - 7g)

$$X_{b,t}^{i,j} \in [0,1], q_{i,b}^{j} \in [-Q_{max}^{j}, Q_{max}^{j}]$$
 $\forall j \in S$

$$X_{b,t}^{i,m,p} \in [0,1], q_{u,b}^p \in [0,\mathcal{Q}_{b,t}^{max}] \qquad \qquad \forall p \in \mathbf{P}$$

$$\Delta b_{b,t}^{p} \in [0, \overline{\Delta b_{b}^{p}}] \qquad \forall p \in \mathbf{P}$$

The objective function minimizes the total operation cost of the JPWNs. The first two terms in the objective function are the fixed costs and the linear costs of the power generating units. The third term is added to minimize the total consumption of electricity needed to pump the water in the network. The last term reflects the purchased water from the reservoirs.

2.4.2 | ACOPF

In order to compare the performance of the proposed cooptimization model under different optimal power flow mechanisms in power network, AC optimal power flow (ACOPF) model is also integrated with the water network by the following constraints.

$$P_{b,t}^{p,new} = \sum_{b=1}^{P} B P_{b,t}^{p} \qquad \forall b, \forall t,$$
 (8a)

$$P_{dn,t} = P_{d,t} + P_{b,t}^{p,new} \qquad \forall n, \forall t,$$
 (8b)

$$\underline{P_{dn}} \le P_{d,t} + P_{b,t}^{p,new} \le \overline{P_{dn}} \qquad \forall n, \forall t, \qquad (8c)$$

$$\sum_{g=1}^{G} P_{g,t} - \sum_{m \in \Omega_{l}^{n}} P_{knm,t} = P_{dn,t} \qquad \forall n, \forall t, \qquad (8d)$$

$$\sum_{\varrho \in G_{i}} P_{g,t} - \sum_{d \in D_{i}} P_{dn,t} = \sum_{k \in K_{e}} P_{k,t} - \sum_{k \in K_{e}} P_{k,t} \quad \forall t, \quad (8e)$$

$$\sum_{g \in G_i} \mathcal{Q}_{g,t} - \sum_{d \in D_i} \mathcal{Q}_{d,t} = \sum_{k \in K_i} \mathcal{Q}_{k,t} - \sum_{k \in K_i} \mathcal{Q}_{k,t} \quad \forall t, \quad (8f)$$

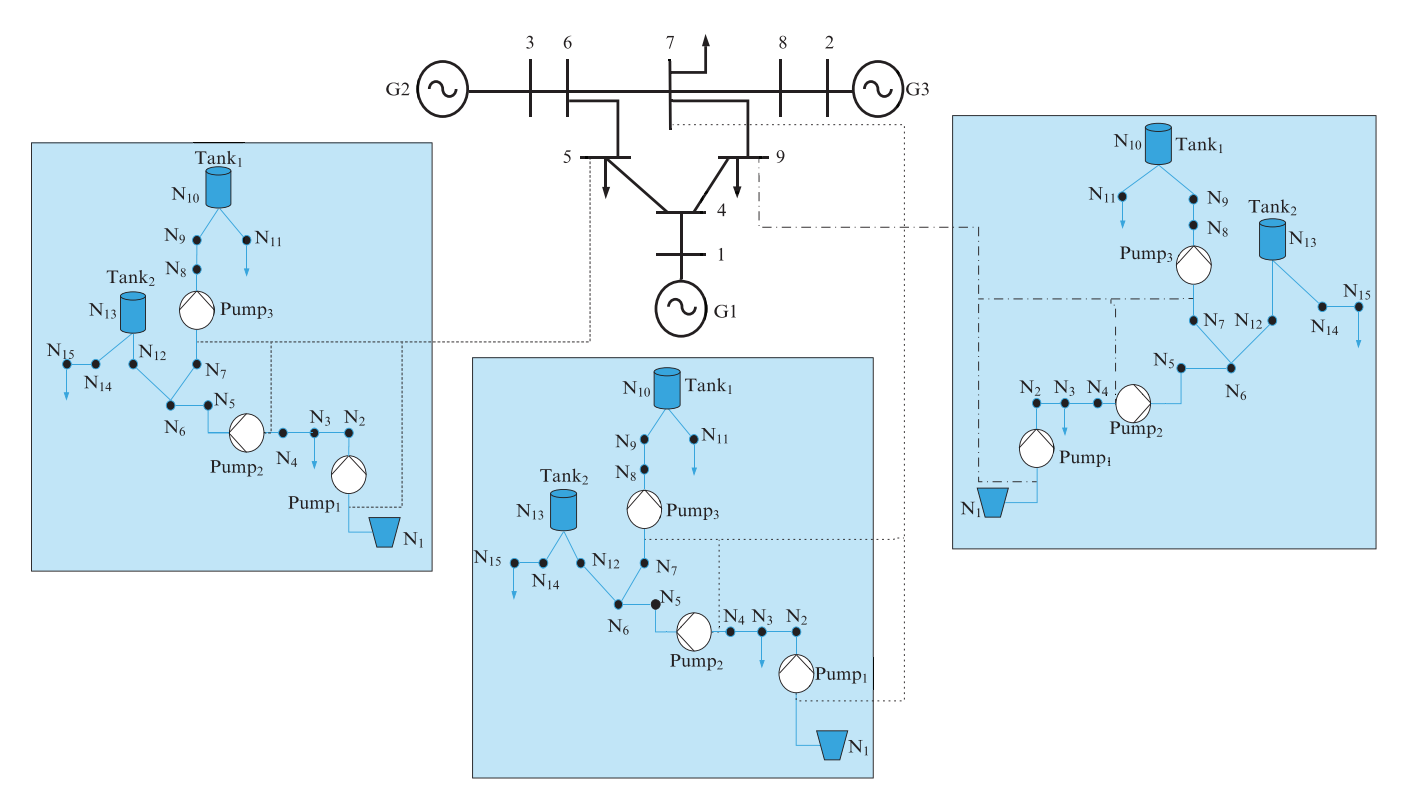


FIGURE 3 Schematic diagram of the 9-bus test system integrated with three water networks

$$P_{k,t} = (\Delta V_{i,t} - \Delta V_{j,t})g_k - b_k \theta_{k,t} \qquad \forall i, \forall t,$$
 (8g)

$$Q_{k,t} = -(1+2\Delta V_{i,t})b_{k0} - (\Delta V_{i,t} - \Delta V_{j,t})b_k - g_k\theta_{k,t} \quad \forall i, \forall t,$$
(8h)

$$-0.05 \le \Delta V_{i(j),t} \le 0.05 \qquad \forall i(j), \forall t, \qquad (8i)$$

$$-\frac{\pi}{2} \le \theta_{k,t} \le \frac{\pi}{2} \qquad \forall k, \forall t. \tag{8j}$$

Constraints (8a–8c) integrate the total electricity demand consumed by water and power systems at each bus. The active and reactive power balance between the generation and loads in all nodes are enforced in (8e) and (8f). The active and reactive power flows across transmission lines are characterized through linearized AC power flow as modeled in (8g) and (8h). Voltage magnitude and angle for each node are, respectively, limited in (8i) and (8j).

The complete mixed-integer linear programming (MILP) optimization model of joint operation of the linearized AC optimal power flow integrated with water infrastructure is formulated below:

$$\min \sum_{t=1}^{NT} \sum_{g=1}^{G} \sum_{r=1}^{\mathbf{R}} \sum_{p=1}^{\mathbf{P}} \left(c_{0,t} + c_{g,t} P_{g,t} + c_{p,t} P_{b,t}^p + c_{r,t} \mathcal{Q}_{b,t}^{in} \right)$$

subject to
$$(1a - 1d)$$
, $(2c - 4d)$, $(5c - 6g)$, $(8a - 8j)$

$$X_{b,t}^{i,j} \in [0,1], q_{i,b}^j \in [-Q_{max}^j, Q_{max}^j]$$
 $\forall j \in S$

$$X_{b,t}^{i,m,p} \in [0,1], q_{u,b}^p \in [0,\mathcal{Q}_{b,t}^{max}] \qquad \qquad \forall p \in \mathbf{P}$$

$$\Delta b_{b,t}^{p} \in [0, \overline{\Delta b_{b}^{p}}] \qquad \forall p \in \mathbf{P}$$

3 | NUMERICAL CASE STUDIES

3.1 | System descriptions, data, and assumptions

The proposed formulation for the joint operation optimization of the interdependent power and water systems is implemented on the IEEE 9-bus test system connected to three water networks as illustrated in Figure 3. The 9-bus test system consists of three generating units, nine transmission lines, and three load points. Each water network consists of 15 nodes and is connected to a power grid load point. Note that each water system includes 11 pipelines, 3 pumps, and 2 tanks. Water demands are located at nodes 3, 11, and 15 for each water system. Details on the location of each component in the water network (e.g. pumping stations, water tanks, nodes etc.) are demonstrated in each blue box in Figure 3. Reservoir is treated here as an unlimited source of water and tanks are set to be empty at the initial time. In this model, each water system is characterized with identical parameters (e.g. tank volume, demands etc.). All system data (i.e. the hourly generation and load profiles, transmission

line parameters, water demand, pipeline parameters etc.) are provided in [36]. All simulations are performed in A Mathematical Programming Language (AMPL) environment [37], using a PC with an Intel Xeon E5-2620 v2 processor, 16 GB of memory, and 64-bit operating system. CPLEX solver is used to simulate and solve the reformulated MILP model.

3.2 | Results and discussions

In order to illustrate the performance of the proposed optimization model, four different test cases (TC) are studied.

- Test Case 1 (TC1) presents the classic approach for the operation of PWNs, which assumes that the use of electricity for water pumps (water network operation) and the DCOPF mechanism (power network operation) are individually optimized by two independent operators in respective domains. As the conventional practice (benchmark), the optimization model in TC1 is conducted in two steps. First, water system operators optimize the electricity usage of water pumps as well as the purchased water at each time interval and send the estimated electricity demand in the water sector to power system operators. Next, DCOPF is performed by power system operators considering the electricity demand requested to operate the water pumps.
- Test Case 2 (TC2) represents the proposed framework in which water and power systems are jointly and interdependently operated (i.e. JPWN) where DCOPF and water hydraulic constraints are efficiently merged. The optimization engine in TC2 runs only once by a single JPWN operator.
- Test Case 3 (TC3) presents the classic approach for the operation of PWNs (benchmark) and studies the optimization of ACOPF and water hydraulic constraints, individually approached by two independent operators and optimized in two steps as in TC1.
- Test Case 4 (TC4) models the proposed integration of the hydraulic constraints in water systems and the ACOPF constraints in power systems, where both systems are jointly and interdependently operated, thereby enabling the operation benefits of JPWNs.

The operation costs comparison between the classic operation approach for PWNs (TC1 and TC3) and the proposed operation of JPWNs (TC2 and TC4) is shown in Table 1. TC1 results in a total operation cost of \$38,419.55 for water and power system operation, while in TC2, the optimal operation cost for the JPWN is reported \$20,174.71. TC3 results in a total cost of \$42,287.04 for the two-step independent operation of the water and power systems, while the optimal cost for the JPWN in TC4 is found \$21,527.71. Comparing the total operation cost using DCOPF-based operation mechanism in TC1 (traditional approach) with that proposed in TC2, one can observe that TC2 yields more efficient outcomes in terms of the total operation cost saving, where the cost has been reduced by 18,244.84\$. For the ACOPF-based operation mechanism applied in TC3 and TC4, the operation cost is lower by

TABLE 1 Summary of the operation cost in different test cases

Test case #	Power system operation cost (\$)	Water system operation cost (\$)	Total operation cost (\$)
TC1	20,377.85	18,041.71	38,419.55
TC3	24,245.33	18,041.71	42,287.04
	Joint Power-Water Ne		
TC2	20,174.71		
TC4	21,527.71		

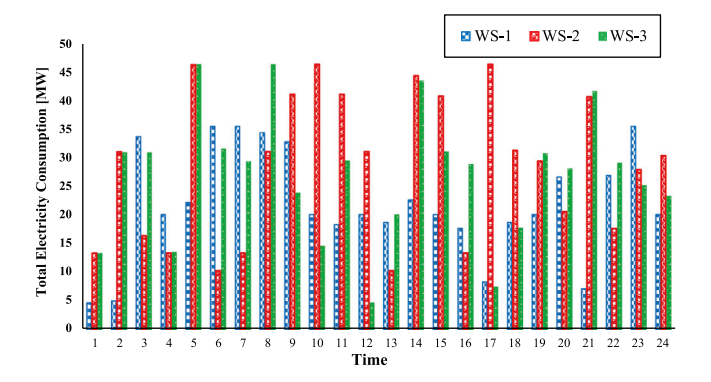


FIGURE 4 Optimal electricity consumption in each water system

20,759.33\$ using the proposed technique. The cost reduction is achieved by optimally operating the electricity-intensive component in the water network (i.e. pumps) and optimally capturing the availability of tanks within the JPWN operation. One can see, from the reported results, that the suggested methodology enhances the economic efficiency of the interconnected networks.

The energy consumption in each water network for all test cases are provided in Figures 4–6. Figure 4 demonstrates the required electricity demand for the operation of the three water systems submitted by the water system operators to power system operator in TC1 and TC3 in which the operation of water and power systems are independently optimized. For DCOPF-based operations in TC1 and TC2, Figure 5 specifies the total energy consumption for each water network. Figure 5 shows that the total electricity consumption from the water network

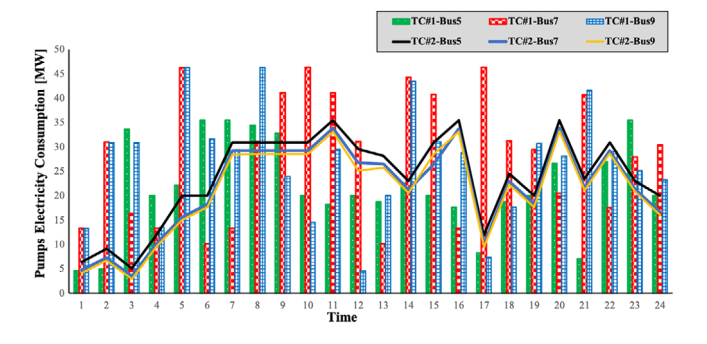


FIGURE 5 Water networks performance in DCOPF-based operation models in TC1 and TC2

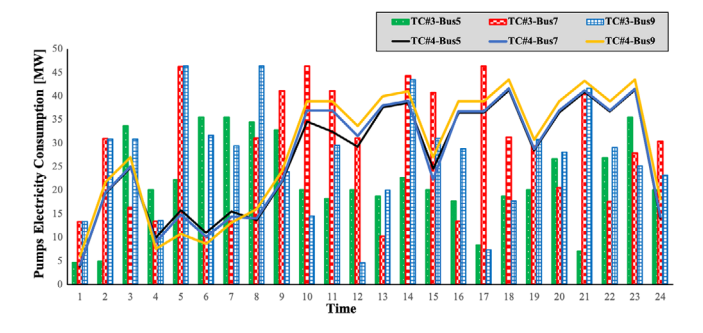


FIGURE 6 Water networks performance in ACOPF-based operation models in TC3 and TC4

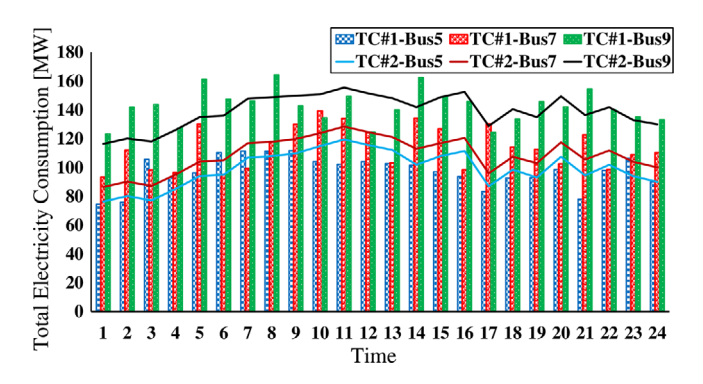


FIGURE 7 Total power-water demand at each coupled node considering DCOPF in TC1 and TC2

using the proposed JPWN approach (TC2) is lower compared to the traditional practice of operating the two networks individually (TC1). When ACOPF-based operation mechanism is applied in TC3 and TC4, Figure 6 illustrates that our proposed JPWN optimization model (TC4) reduces the electricity consumed by the water network compared to that in TC3, where the two systems are independently optimized.

The total load profile in the IEEE 9-bus test system is analysed in Figures 7 and 8 when DCOPF and ACOPF formulations are applied. For DCOPF operations in TC1 and TC2, Figure 7 illustrates the load profile for three different water systems supplied by the studied power system at load point 5, 7, and 9. According to Figure 7 where the DCOPF is applied, it can be

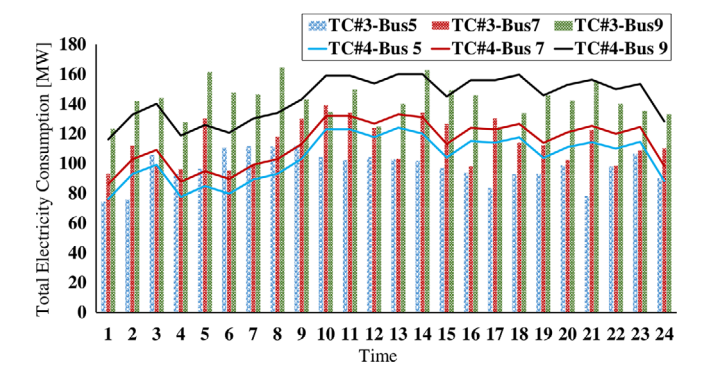


FIGURE 8 Total power-water demand at each coupled node considering ACOPF in TC3 and TC4

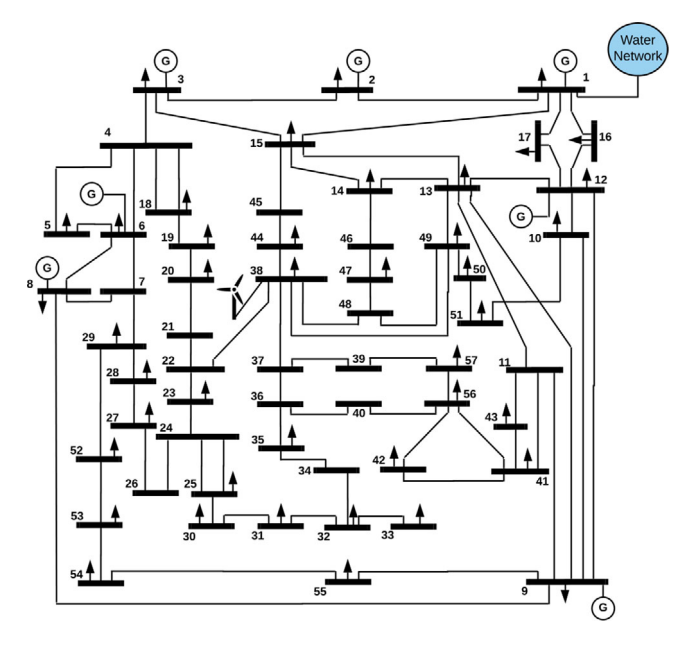


FIGURE 9 Schematic diagram of the IEEE 57-bus test system integrated with water networks

TABLE 2 Summary of the computational time in two test systems

IEEE-9 bus test system		IEEE-57 bus test system	
Test Case #	Time (s)	Test Case #	Time (s)
TC1	66.1	TC1	100.94
TC2	85.4	TC2	131.4
TC3	67.6	TC3	104.2
TC4	91.07	TC4	140.1

seen that the total electricity demand required to operate the water systems, when the two models operate jointly (TC2), is lower compared to a case where both systems are operated separately and independently (TC1). For ACOPF operations in TC3 and TC4, Figure 8 demonstrates that the use of our proposed joint operation optimization model (TC4) reduces the electricity load profile compared to TC3 where the two systems are independently optimized.

To further extend the simulation results and verify the scalability of the proposed approach, the proposed formulations are tested on a larger test system. The IEEE 57-bus test system integrated with the water network (see Figure 9) is used to test the computational complexity of the proposed approach. Table 2 compares the computational times for the IEEE 9-bus test system and the IEEE 57-bus test system integrated with water networks under four different case studies. In the IEEE 9-bus test system, the computational times for TC1 and TC3, where DCOPF- and ACOPF-based operation mechanisms are applied in the decoupled and traditional practice of operating the two networks, are reported 66.1 s and 67.6 s, respectively. The computational times in TC1 and TC3 using the IEEE 57-bus test system are found 100.94 and 104.2 s, respectively. When the

proposed integrated model is applied in TC2 and TC4, the computational times are found 85.4 s and 91.07 s, respectively, for the cases where DCOPF- and ACOPF-based operation mechanisms are employed on the IEEE 9-bus test system. The computational times of the proposed models when applied to a larger system (i.e. IEEE 57-bus test system) are reported 131.4 s in TC2 and 140.1 s in TC4. Even though the computation times for TC1 and TC3 are lower than the proposed model in both test systems, the time needed to coordinate the data exchange between the two networks is not included. The proposed approach in TC2 and TC4 is still computationally attractive for the daily operation of the interconnected networks. Additionally, the results reveal that the proposed analytics are scalable to the larger-scale systems and under real-world scenarios.

4 | CONCLUSION

Different from the state-of-the-art research, this paper has presented a holistic framework for day-ahead joint operation optimization of the interdependent water and power systems by an independent system operator. The integration of OPF mechanisms (both DC and AC settings) in power systems with hydraulic water system operation has been taken into account to evaluate the proposed framework's applicability and effectiveness in managing the interdependent critical infrastructure. The piece-wise linearization technique was used to approximate the nonlinear functions of the water pumping operations as well as the pressure head loss between different nodes in the water network. Hence, the non-convex optimization is transformed to a tractable mixed-integer linear programming (MILP) formulation that can be quickly solved by commercial off-the-shelf solvers. The simulation results on the 15-node water network jointly operated with the IEEE 9-bus test power system revealed that the proposed analytics for joint operation co-optimization of interdependent water and power infrastructures significantly lower the total operating costs. This is achieved through optimizing the electricity consumption by electric pumps used in the water networks and storing water in tanks during the peak electricity demand time intervals. The scalability of the proposed framework is also tested on a large test system, that is, the IEEE 57-bus test system connected to a 15node water network, and the results verified that the proposed methodology is scalable and computationally efficient.

ACKNOWLEDGEMENTS

This work was supported in part by the U.S. National Science Foundation (NSF) under Grant CNS-1951847.

NOMENCLATURE

 $[n \in \Omega_B]$ Set of electric system buses.

 $[g \in \Omega_G]$ Set of power generating units.

 $[k \in \Omega_L]$ Set of power system transmission lines.

 $[r \in \mathbf{R}]$ Set of water system reservoirs.

 $[p \in \mathbf{P}]$ Set of water system pumps.

 $[j \in S]$ Set of water system pipes.

Parameters and constants

 $[P_{d,t}]$ Total electricity demand at time t (MW).

 $[\overline{P_{dn}}, P_{dn}]$ Maximum/Minimum electricity demand.

 $[x_k]$ Reactance of transmission line k.

 $[P_k^{max}]$ Maximum power flow limit of line k (MW).

 $[P_g^{max}]$ Maximum capacity limit of generating unit g.

 $[P_g^{min}]$ Minimum capacity limit of generating unit g.

 $[g_k]$ Conductance of transmission line k.

 $[b_k]$ Series admittance of transmission line k.

 $[D_{b,t}]$ Vector of water demand (m^3/b) for each bus b at time t.

 $[\hat{b}_b]$ Reservoirs' geographical height at each bus b.

 $[V_{min,b}]$ Tanks' minimum volume at each bus b.

 $[V_{max,b}]$ Tanks' maximum volume at each bus b.

 $[\Delta E_{min,b}]$ Minimum charging/discharging difference for tanks at each bus b.

 $[\Delta E_{max,b}]$ Maximum charging/discharging difference for tanks at each bus b.

 $[r_b]$ Pipe parameter.

 $[b_{min,b}]$ Minimum nodal pressure heads at each bus b.

 $[b_{max.b}]$ Maximum nodal pressure heads at each bus b.

 $[Q_{max/min,b}]$ Maximum/Minimum water flow rate to the network at each bus b.

 $[P_{max/min,b}^{p}]$ Maximum/Minimum power consumption for pump p at each bus b.

 $[q_{i,b}^p]$ Water flow rate of breakpoint *i* for pump *p* at each bus *b*.

 $[q_{i,b}^j]$ Water flow rate of breakpoint *i* for pipe *j* at each

 $[w_{m,b}^p]$ Pump speed breakpoint *m* at each bus *b*.

 $[c_{0,t}]$ Fixed cost of generating unit g at time t (\$).

 $[c_{g,t}]$ Linear cost of generating unit g at time t (\$/MW).

 $[c_{p,t}]$ Operation cost of pump p at time t.

 $[c_{r,t}]$ Operation cost of reservoir r at time t.

 $[w_{i,b}^p]$ Speed breakpoint *i* for pump *p* at each bus *b*.

 $[a_{1,2,3}, b_{1,2}]$ Performance parameters for pumps.

[B] Incidence matrix of pumps' location.

 $[L_p]$ Pipe length (m).

[g] Gravity (9.8 m/s^2) .

[d] Pipe diameter (m).

Decision variables

 $[Q_{ht}]$ Water flow rate for each bus b at time t.

 $[Q_{b,t}^{m}]$ Vector of reservoirs' water inflow rate for each bus b at time t.

 $[Q_{b,t}^{j}]$ Water flow rate through pipe j for each bus b at time

 $[Q_{b,t}^p]$ Water flow rate through pump p for each bus b at time t.

 $[b_{ht}]$ Pressure heads for each bus b at time t.

 $[b_{b,t}^r]$ Pressure heads associated with reservoir r for each bus b at time t.

[Sign(.)] Sign function.

- $[\Delta E_{b,t}]$ The difference of tanks' inflow/outflow rate for each bus b at time t.
 - $[T_{b,t}^{in}]$ Vector of water inflow to tanks for each bus b at time t.
 - $[T_{b,t}^{out}]$ Vector of water outflow to tanks for each bus b at time t.
 - $[V_{b,t}]$ Volume of stored water in tanks for each bus b at time t.
 - $[W_{b,t}]$ Pumps' speed for each bus b at time t.
 - $[P_{b,t}^p]$ Power consumption for pump p and bus b at time t.
- $[P_{b,t}^{p,new}]$ Vector of water electricity consumption in bus b at time t.
- $[X_{b,t}^{i,j}]$ Continuous decision variable for pressure head breakpoint i associated with pipe j for each bus b at time t.
- $[X_{b,t}^{u,m,p}]$ Continuous decision variable for pressure head breakpoint u associated with pump p for each bus b at time t.
 - $[P_{g,t}]$ Expected power output of generating unit g at time t.
- $[P_{knm,t}]$ Power flow through transmission line k (connecting bus n to bus m) at time t.
 - $[P_{k,t}]$ Active power flow on line k at time t.
- $[Q_{k,t}]$ Reactive power flow on line k at time t.
- $[Q_{g,t}]$ Reactive power of generating unit g at time t.
- $[Q_{d,t}]$ Reactive power of demand d at time t.
- $[\Delta V_{i,t}]$ Voltage magnitude deviation from 1 p.u. at bus *i* at time *t*.
- $[P_{dn,t}]$ Total power-water demand at time t (MW).
- $[\theta_{i,t}]$ Voltage angle for bus *i* at time *t*.

Binary variables

- $[Y_{b,t}^{i,j}]$ Binary variable for pressure head breakpoint i associated with pipe j for bus b at time t.
- $[\beta_{i,m,p,b,t}^{Upper}]$ Binary variable for the upper triangle in the rectangle at time t.
- $[\beta_{i,m,p,b,t}^{Lower}]$ Binary variable for the lower triangle in the rectangle at time t.

ORCID

Mohannad Alhazmi https://orcid.org/0000-0002-3031-4380

REFERENCES

- Leiby, V.M., Burke, M.E: Energy Efficiency Best Practices for North American Drinking Water Utilities. Water Research Foundation, Denver (2011)
- Appelbaum, B., et al.: Water & Sustainability: US Electricity Consumption for Water Supply & Treatment—The Next Half Century. Electric Power Research Institute, Palo Alto (2002)
- 3. Shin, S., et al.: A systematic review of quantitative resilience measures for water infrastructure systems. Water 10(2), 164 (2018)
- Li, Q., et al.: Modeling and co-optimization of a micro water-energy nexus for smart communities. In: 2018 IEEE PES Innovative Smart Grid Technologies Conference Europe (ISGT-Europe), pp. 1–5. IEEE, Piscataway (2018)
- Zhang, X., Vesselinov, V.V.: Energy-water nexus: Balancing the tradeoffs between two-level decision makers. Appl. Energy 183, 77–87 (2016)

- Santhosh, A., et al.: Real-time economic dispatch for the supply side of the energy-water nexus. Appl. Energy 122, 42–52 (2014)
- Kao, S.-C., et al.: Projecting changes in annual hydropower generation using regional runoff data: An assessment of the United States federal hydropower plants. Energy 80, 239–250 (2015)
- Vakilifard, N., et al.: The role of water-energy nexus in optimising water supply systems—Review of techniques and approaches. Renew. Sustain. Energy Rev. 82, 1424–1432 (2018)
- Fang, D., Chen, B.: Linkage analysis for the water–energy nexus of city. Appl. Energy 189, 770–779 (2017)
- Santhosh, A., et al.: The impact of storage facility capacity and ramping capabilities on the supply side economic dispatch of the energy–Water nexus. Energy 66, 363–377 (2014)
- Santhosh, A., et al.: Optimal network flow for the supply side of the energy-water nexus. In: 2013 IEEE International Workshop on Inteligent Energy Systems (IWIES), pp. 155–160. IEEE, Piscataway (2013)
- Zhang, H., et al.: Daily hydrothermal scheduling with economic emission using simulated annealing technique based multi-objective cultural differential evolution approach. Energy 50, 24–37 (2013)
- Lubega, W.N., Farid, A.M.: Quantitative engineering systems modeling and analysis of the energy–Water nexus. Appl. Energy 135, 142–157 (2014)
- Oikonomou, K., et al.: Optimal demand response scheduling for water distribution systems. IEEE Trans. Ind. Inf. 14(11), 5112–5122 (2018)
- Oikonomou, K., Parvania, M.: Optimal coordination of water distribution energy flexibility with power systems operation. IEEE Trans. Smart Grid 10(1), 1101–1110 (2018)
- Gonzalez, J.M., et al.: Spatial and sectoral benefit distribution in waterenergy system design. Appl. Energy 269, 114794 (2020)
- Zuloaga, S., et al.: Resilience of cyber-enabled electrical energy and water distribution systems considering infrastructural robustness under conditions of limited water and/or energy availability. IEEE Trans. on Eng. Management (2019)
- Thompson, L.: Automated Demand Response Opportunities in Wastewater Treatment Facilities. Lawrence Berkeley National Laboratory, Berkeley (2008)
- Pabi, S., et al.: Electricity Use and Management in the Municipal Water Supply and Wastewater Industries, vol. 194. Electric Power Research Institute, Palo Alto (2013)
- Sparn, B., Hunsberger, R.: Opportunities and challenges for water and wastewater industries to provide exchangeable services. Technical Report. National Renewable Energy Laboratory, Golden (2015)
- Siddiqui, O.: Assessment of Achievable Potential from Energy Efficiency and Demand Response Programs in the US (2010–2030), pp. 2010–2030.
 Electric Power and Research Institute, Palo Alto (2009)
- Fooladivanda, D., et al.: Utilization of water supply networks for harvesting renewable energy. IEEE Trans. Control Network Syst. 6(2), 763–774 (2018)
- Li, Q., et al.: Micro water–energy nexus: Optimal demand-side management and quasi-convex hull relaxation. IEEE Trans. Control Network Syst. 6(4), 1313–1322 (2018)
- Zamzam, A.S., et al.: Optimal water–power flow-problem: formulation and distributed optimal solution. IEEE Trans. Control Network Syst. 6(1), 37– 47 (2018)
- Alhazmi, M., et al.: Joint operation optimization of the interdependent water and electricity networks. In: 2020 IEEE Industry Applications Society ety Annual Meeting, pp. 1–7. IEEE, Piscataway (2020)
- Santhosh, A., et al.: Optimal network flow for the supply side of the energy-water nexus. In: 2013 IEEE International Workshop on Inteligent Energy Systems (IWIES), pp. 155–160. IEEE, Piscataway (2013)
- Stuhlmacher, A., Mathieu, J.L.: Chance-constrained water pumping to manage water and power demand uncertainty in distribution networks. Proc. IEEE 108(9), 1640–1655 (2020)
- Stuhlmacher, A., Mathieu, J.L: Chance-constrained water pumping managing power distribution network constraints. In: 2019 North American Power Symposium (NAPS), pp. 1–6. IEEE, Piscataway (2019)
- Zhao, P., et al.: Water-energy nexus: A mean-risk distributionally robust co-optimization of district integrated energy systems. IEEE Trans. Power Syst. (2020)

- Kurek, W., Ostfeld, A.: Multi-objective optimization of water quality, pumps operation, and storage sizing of water distribution systems. J. Environ. Manage. 115, 189–197 (2013)
- Bragalli, C. et al.: On the optimal design of water distribution networks: a practical minlp approach. Optim. Eng. 13(2), 219–246 (2012)
- 32. Brown, P., et al.: Hurricanes and the environmental justice island: irma and maria in puerto rico. Environ. Justice 11(4), 148–153 (2018)
- 33. Subramanian, R., et al.: Air quality in puerto rico in the aftermath of hurricane maria: a case study on the use of lower cost air quality monitors. ACS Earth Space Chem. 2(11), 1179–1186 (2018)
- 34. Lin, Y., et al.: Impact of hurricane maria on drinking water quality in puerto rico. Environ. Sci. Technol. 54(15), 9495–9509 (2020)
- 35. D'ambrosio, C., et al.: Piecewise linear approximation of functions of two variables in milp models. Oper. Res. Lett. 38(1), 39–46 (2010)

- Data information. http://tiny.cc/GWU-SmartGridLab. Accessed 30 Sept 2020
- Fourer, R., et al.: AMPL: A Modeling Language for Mathematical Programming. Brooks/Cole, Belmont (1993)

How to cite this article: Alhazmi M, Dehghanian P. Optimal integration of interconnected water and electricity networks. IET Gener. Transm. Distrib. 2021;15:2033–2043.

https://doi.org/10.1049/gtd2.12153